Contract No:

This document was prepared in conjunction with work accomplished under Contract No. DE-AC09-08SR22470 with the U.S. Department of Energy.

HYDROGEN EFFECTS ON STRAIN-INDUCED MARTENSITE FORMATION IN TYPE 304L STAINLESS STEEL

Michael J. Morgan, Poh-Sang Lam
Savannah River National Laboratory, Aiken, SC, USA

Dean A. Wheeler
PCC Airfoils, Minerva, OH, USA

INTRODUCTION

Unstable austenitic stainless steels undergo a strain-induced martensite transformation. The effect of hydrogen on this transformation is not well understood. Some researchers believe that hydrogen makes the transformation to martensite more difficult because hydrogen is an austenite stabilizer. Others believe that hydrogen has little or no effect at all on the transformation and claim that the transformation is simply a function of strain and temperature [1-4]. Still other researchers believe that hydrogen should increase the ability of the metal to transform due to hydrogen-enhanced dislocation mobility and slip planarity [5, 6]. While the role of hydrogen on the martensite transformation is still debated, it has been experimentally verified that this transformation does occur in hydrogen-charged materials [1-7].

What is the effect of strain-induced martensite on hydrogen embrittlement? Martensite near crack-tips or other highly strained regions could provide much higher hydrogen diffusivity and allow for quicker hydrogen concentration [8-10]. Martensite may be more intrinsically brittle than austenite and has been shown to be severely embrittled by hydrogen [1]. However, it does not appear to be a necessary condition for embrittlement since Type 21-6-9 stainless steel is more stable than Type 304L stainless steel but susceptible to hydrogen embrittlement [1].

In this study, the effect of hydrogen on strain-induced martensite formation in Type 304L stainless steel was investigated by monitoring the formation of martensite during tensile tests of as-received and hydrogen-charged samples and metallographically examining specimens from interrupted tensile tests after increasing levels of strain. The effect of hydrogen on the fracture mechanisms was also studied by examining the fracture features of as-received and hydrogen-charged specimens and relating them to the stress-strain behavior.

EXPERIMENTAL PROCEDURE

Tensile specimens were machined from the plate grade Type 304L stainless steel having the composition shown in Table 1. The specimen axis was aligned parallel to the rolling direction. Samples were exposed to 69 MPa of hydrogen gas at 350 C for three weeks. The treatment was designed to saturate the samples with hydrogen and the hydrogen concentration was estimated to be 5500 atomic parts per million by using the solubility values of San Marchi, et al. [11]. As-received and hydrogen-charged samples were tested at room temperature in air at an initial strain rate of 1 x 10^{-4} / sec. The formation of strain-induced α' (alpha-prime) martensite during the tensile test was monitored by recording the change in the magnetic phase of the sample by using a ferrite meter mounted to the center of the tensile specimen. The meter was calibrated by using a mild steel sample (100% bcc phase) with a maximum ferrite # of 30.0. In addition, the amount of martensite transformed was qualitatively determined by metallography after interrupted tensile tests.

TABLE 1: COMPOSITIONS OF STAINLESS STEEL FORGINGS (WEIGHT %)

	Cr	Ni	Mn	Mo	C	Si	P	S	N	Co	O	Cu
Type 304L Heat V73204	18.24	8.19	1.85	.33	.018	.36	.028	.004	.073	.14	.002	.21

RESULTS

Figure 1 shows a comparison of the stress-strain behavior for the as-received and hydrogen charged specimens. Internal hydrogen increased the yield strength of the steel by about 10% and decreased the elongation by 66%. The hydrogen-charged sample failed suddenly prior to necking at a stress value that was lower than the ultimate strength of the uncharged sample which necked down prior to failure. This suggests a fracture mode controlled by a critical stress. The uncharged samples showed a large reduction in area and a prominent necked region. The hydrogen-charged specimens showed much smaller reduction-in-area, almost no necking, and numerous secondary cracks on the specimen surface (Fig. 2).

Figure 3 shows the fracture modes of the uncharged and hydrogen-charged samples. Uncharged samples failed by dimpled rupture (Fig. 3a) while charged samples had two distinct fracture features. Twin-boundary parting characterized by large, flat facets, extending over one grain only, was interspersed within larger regions of quasi-cleavage (Fig. 3b). Traces of deformation bands in the underlying grain could be seen on many of the large flat facets, another characteristic of twin-boundary parting [1-3]. The quasi-cleavage fracture appearance was most likely due to hydrogen-induced separation along austenite-martensite interfaces [3] or deformation bands [8].

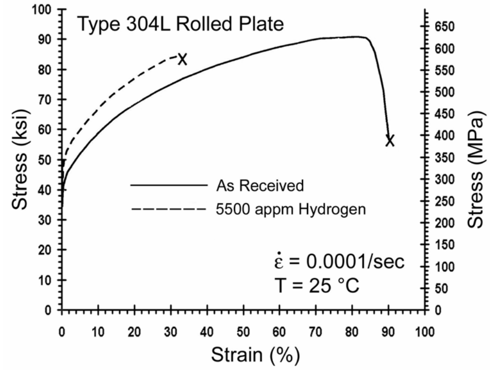

Figure 1: Comparison of Tensile Behavior for the Type 304L Stainless Steel Specimens in the As-Received and Hydrogen-Charged Conditions. Uncharged Samples Necked Down before Failure; Charged Samples Failed before Necking as Indicated by the "x".

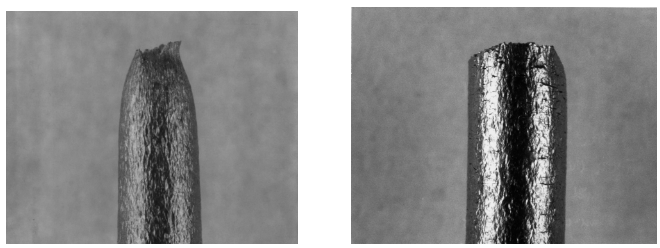

(a) **(b)**

Figure 2: Comparison of Fractured Tensile Specimens in the (a) As-Received and (b) Hydrogen-Charged Conditions.

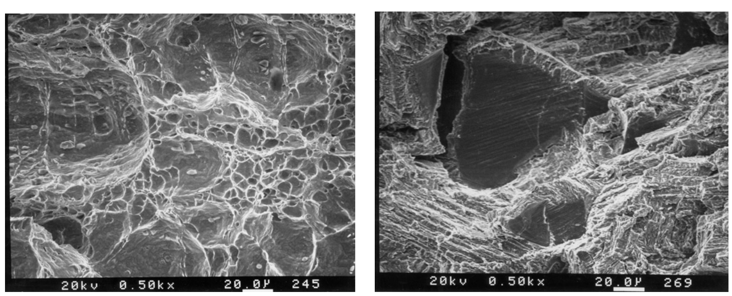

(a) **(b)**

Figure 3: Comparison of Fracture Appearance of Tensile Specimens in the (a) As-Received and (b) Hydrogen-Charged Conditions.

Figure 4 shows the results of the in-situ measurement of transformed martensite during the tensile tests. The results suggest that hydrogen charged samples had slightly less transformed martensite than the uncharged samples. The results are different than those of Caskey at ambient temperature, which indicated that hydrogen caused a slight increase in strain-induced martensite in Type 304L stainless steel [3]. However, the results of Fig. 4 are misleading because the samples did not always fail in the center of the gage section, where the ferrite probe was mounted. Measurements after the tensile test indicated that ferrite was higher at the point of fracture than it was at the center of the gage.

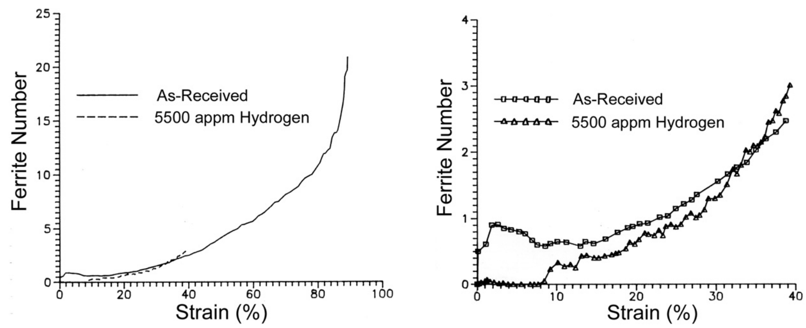

Figure 4: Increase in Ferrite Number with Increasing Strain during Tensile Test for As-Received and Hydrogen-Charged Samples. Low Strain Region on Right.

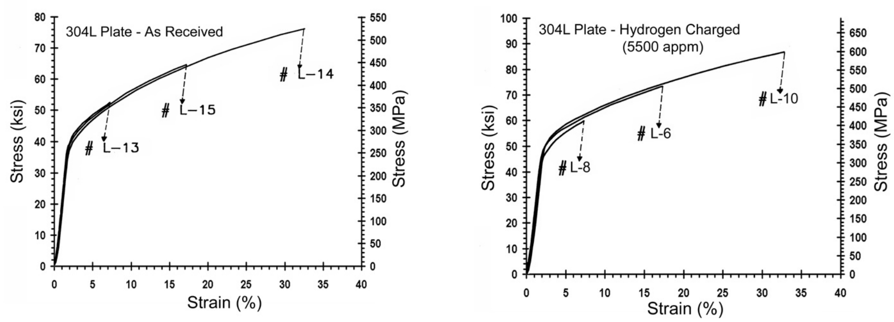

(a) **(b)**

Figure 5: Tensile Specimens were interrupted at Plastic Strain Values of 5, 15, and 30% and Metallographically Examined: (a) As-Received and (b) Hydrogen-Charged

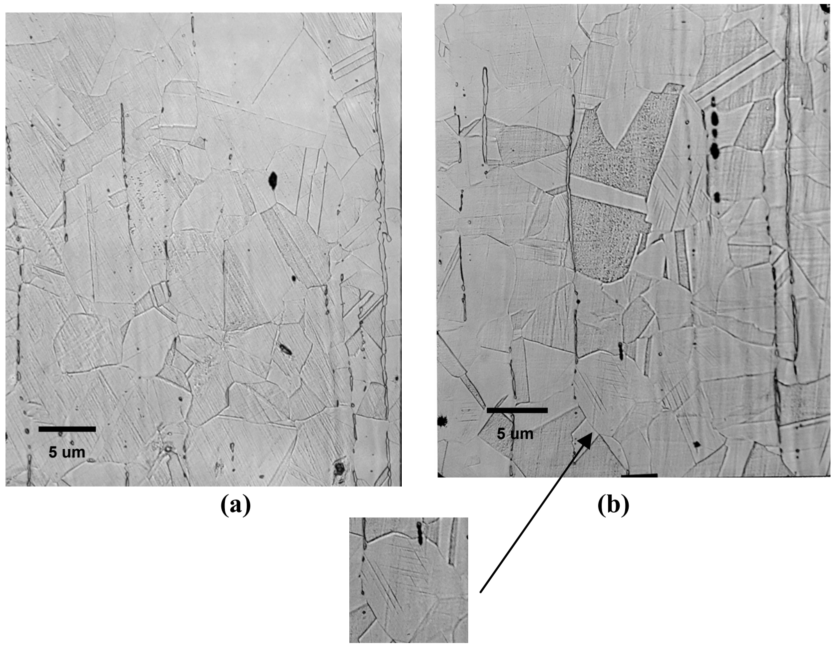

Figure 6: Tensile Specimens Interrupted after 5% Plastic Strain: (a) As-Received and (b) Hydrogen-Charged. Inset Shows Transformed Martensite.

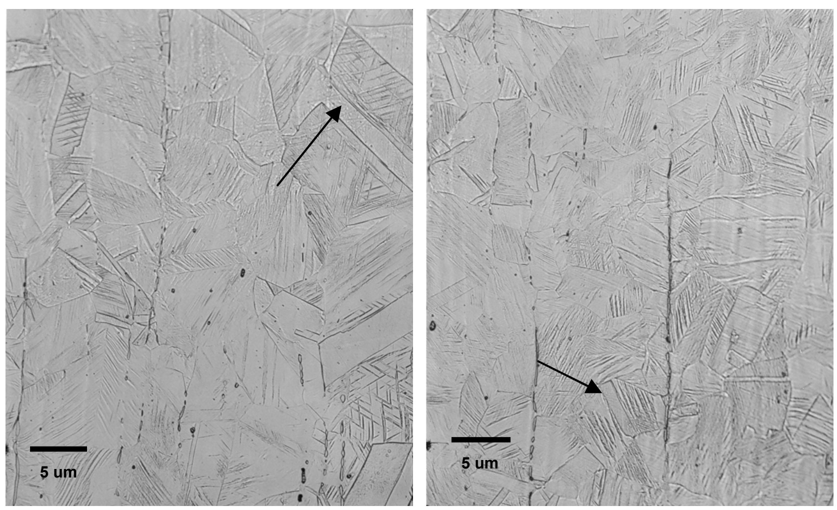

(a) **(b)**

Figure 7: Tensile Specimens Interrupted after 30 % Plastic Strain: (a) As-Received and (b) Hydrogen-Charged. Arrows Indicate Feathery Appearance of Transformed Martensite.

Metallographic examination of interrupted tensile tests (Figures 5-7) indicates that hydrogen slightly increases the amount of transformed martensite at equivalent levels of plastic strain. Little or no martensite was seen in the elastically strained samples. At low levels of plastic strain ($\varepsilon_p < 5\%$), a very small amount of martensite could be seen in the center of few grains for the hydrogen-exposed samples (Fig. 6). No martensite was seen in the unexposed sample at this level of plastic strain (Fig. 6). For higher levels of plastic strain (up to 30% ε_p), the hydrogen-exposed samples had slightly more transformed martensite than the unexposed samples (Fig. 7). In total, the metallographic observations did not indicate a very strong effect of hydrogen on the amount of strain-induced martensite in this steel.

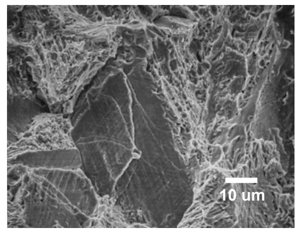

Figure 8: Hydrogen-Charged Sample Fracture Features. A Particle in the Center of the Twin Boundary Facet Apparently Acted as a Crack Nucleus.

DISCUSSION

The stress-strain tests did not indicate a very strong effect of hydrogen on the amount of strain-induced martensite. However, they did indicate a rather dramatic effect of hydrogen on the fracture behavior. The fracture surfaces of the hydrogen-charged specimens revealed two distinctly different fracture features (Fig. 3b). Isolated, flat twin-boundary facets were separated by more ductile features like dimpled rupture and quasi-cleavage fracture. The microvoids in the dimpled rupture areas were much smaller and more closely spaced than the microvoids on the as-received sample fracture surfaces. The quasi-cleavage fracture modes were only seen in the hydrogen-charged samples. Figure 8 shows that at least some of the twin boundary facets contained particles that apparently act as crack nuclei.

The stress-strain behavior of the hydrogen-charged samples was different than the as-received sample behavior as well. Hydrogen-charged samples tended to fail well after yield and just at or after maximum load. The maximum load point was very sharp, unlike the as-received samples which tended to show a much more smooth and rounded-off stress strain curve at maximum load and beyond. Caskey reports numerous twin boundary microcracks oriented transverse to the tensile axis in longitudinal sections of tensile specimens [3].

Together, these observations suggest that, in hydrogen-charged samples, the twin-boundaries are weakened by hydrogen and separate after some amount of plastic strain. High local stresses from deformation bands intersecting the twin boundaries may be needed to separate the weakened twin-boundary interface. After nucleation of numerous microcracks in the gage section of the tensile sample, the effective cross-sectional area would be substantially reduced, which would lead to the fast, overload fracture of the remaining ligaments as shown schematically in Fig. 9. The fast overload fracture regions of the hydrogen-charged samples were dominated by a quasi-cleavage fracture appearance.

What is the role of martensite formation on this fracture mode? Hydrogen may have slightly increased the amount of strain-induced martensite at any given level of strain.
The formation of flat facets has been related to the cracking of twin boundaries [12-14]. Strain-induced martensite was not evident on the fracture surfaces of the uncharged samples (Fig. 3a). On the other hand, a significant increase in the extent of quasi-cleavage fracture was observed on the fracture surfaces of hydrogen-charged samples (Fig. 3b). Apparently, the ligaments between the areas of cracked twin boundaries separate along the austenite-martensite interfaces or deformation bands when hydrogen is present in the steel, resulting in the quasi-cleavage appearance. Thus, cracking of hydrogen weakened twin boundary interfaces and hydrogen-induced quasi-cleavage of the ligaments between the fractured twin boundaries results in the marked reduction in elongation (Fig. 1).

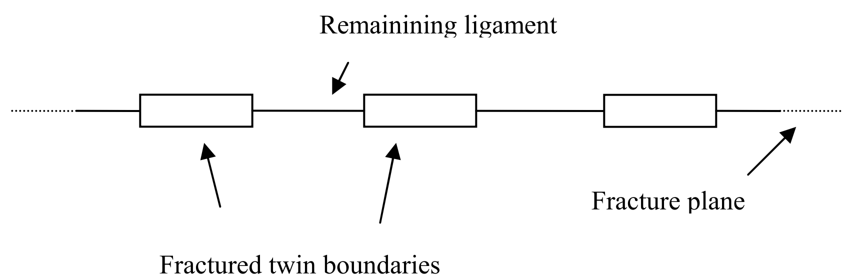

Figure 9: Schematic showing the apparent fracture mechanism of hydrogen-charged samples.

SUMMARY

Tensile tests showed that hydrogen-charged samples had higher yield strengths, lower elongations and different fracture modes than uncharged samples. Metallographic observations indicate that hydrogen-charged samples had slightly more material transformed to martensite than uncharged samples at equivalent levels of strain. Uncharged samples failed by the microvoid nucleation and growth process. Hydrogen-charged samples failed by isolated twin-boundary cracking near maximum load followed by quasi-cleavage of transformed martensite of the ligaments between the twin-boundary facets.

ACKNOWLEDGMENTS

This document was prepared in conjunction with work accomplished under Contract No. DE-AC09-08SR22470 with the U. S. Department of Energy.

REFERENCES

1. G. R. Caskey, Jr., "Hydrogen Effects in Stainless Steels", Hydrogen Degradation of Ferrous Alloys, ed. J. P. Hirth, R. W. Oriani, and M. Smialowski, eds., (Park Ridge, NJ: Noyes Publication, 1985), p. 822.
2. G. R. Caskey, Jr., "The Role of Twinning and Transformation in Hydrogen Embrittlement of Austenitic Stainless Steels", Environmental Degradation of Engineering Materials, (M. R. Louthan and R. P. McNitt, eds.), pp. 437-450, Virginia Polytechnic Institute, Blacksburg, VA (1977).
3. G. R. Caskey, Jr., "Hydrogen Compatibility Handbook for Stainless Steels", E. I. du Pont de Nemours & Co., Savannah River Laboratory, Aiken, SC 29808, DP-1643, June, 1983.
4. A. W. Thompson and O. Buck, *Metall. Trans.,* Vol. 7A (1976), pp. 329-331.
5. M. R. Louthan, G. R. Caskey, J. A. Donovan, and D. E. Rawl, *Materials Science and Engineering,* Vol. 10 (1972), pp. 357-68.
6. A. W. Thompson, *Metall. Trans*, Vol. 4 (1973), pp. 2819-25.
7. C. Pan, W. Y. Chu, Z. B. Li, D. T. Liang, Y. J. Su, K. W. Gao, L. J. Qiao, *Materials Science and Engineering,* Vol. A351 (2003), pp. 293-298.
8. D. G. Ulmer and C. J. Altstetter, "Mechanism For Hydrogen Embrittlement of Austenitic Stainless Steels", Proc. Fourth Int. Conf. on Hydrogen Effects on Material Behavior, ed. A. W. Thompson and N. R. Moody, (Warrendale, PA: The Minerals, Metals & Materials Society, 1989), p. 421.
9. T. P. Perng and C. J. Alstetter, "Effects of Deformation on Hydrogen Permeation in Austenitic Stainless Steels", *Acta Met*, Vol. 34 (1986), p. 1771.
10. T. P. Perng, C. J. Altstetter, *Metall. Trans.,* Vol. 19A (1988), p. 145.
11. C. San Marchi, B. P. Somerday and S. L. Robinson, "Permeability, Solubility and Diffusivity of Hydrogen Isotopes in Stainless Steels at High Gas Pressures", *International Journal of Hydrogen Energy*, Vol. 32, Issue 1 (2007), pp. 100-116.
12. W. Y. Chu, J. Yao, C.M. Hsiao, *Metall. Trans. A,* Vol. 15 (1980), p. 729.
13. H. Hanninen and T. Hakarainer, *Corrosion*, Vol. 36 (1980), p. 47.
14. G. H. Yu, Y. H. Cheng, L. J. Chen, W.Y. Chu, *Corrosion*, Vol. 53 (1997), p. 762.